PHYSICAL REVIEW B **93**, 060408(R) (2016)

Resonance-inclined optical nuclear spin polarization of liquids in diamond structures

Q. Chen,[1,2,*] I. Schwarz,[1,2] F. Jelezko,[2,3] A. Retzker,[4] and M. B. Plenio[1,2]

[1]*Institut für Theoretische Physik, Universität Ulm, Albert-Einstein-Allee 11, 89069 Ulm, Germany*

[2]*IQST, Universität Ulm, Albert-Einstein-Allee 11, 89069 Ulm, Germany*

[3]*Institut für Quantenoptik, Universität Ulm, 89073 Ulm, Germany*

[4]*Racah Institute of Physics, The Hebrew University of Jerusalem, Jerusalem 91904, Israel*

(Received 13 October 2015; revised manuscript received 3 February 2016; published 24 February 2016)

Dynamic nuclear polarization (DNP) of molecules in a solution at room temperature has the potential to revolutionize nuclear magnetic resonance spectroscopy and imaging. The prevalent methods for achieving DNP in solutions are typically most effective in the regime of small interaction correlation times between the electron and nuclear spins, limiting the size of accessible molecules. To solve this limitation, we design a mechanism for DNP in the liquid phase that is applicable for large interaction correlation times. Importantly, while this mechanism makes use of a resonance condition similar to solid-state DNP, the polarization transfer is robust to a relatively large detuning from the resonance due to molecular motion. We combine this scheme with optically polarized nitrogen-vacancy (NV) center spins in nanodiamonds to design a setup that employs optical pumping and is therefore not limited by room temperature electron thermal polarization. We illustrate numerically the effectiveness of the model in a flow cell containing nanodiamonds immobilized in a hydrogel, polarizing flowing water molecules 4700-fold above thermal polarization in a magnetic field of 0.35 T, in volumes detectable by current NMR scanners.

DOI: 10.1103/PhysRevB.93.060408

Introduction. Nuclear spin hyperpolarization, i.e., a population difference between the nuclear spin states that exceeds significantly the thermal equilibrium value, is a key emerging method for increasing the sensitivity of nuclear magnetic resonance (NMR) [1,2] which is proportional to the sample polarization. By enhancing the magnetic resonance signals by several orders of magnitude, a wide range of novel applications in biomedical sciences are made possible, such as metabolic MR imaging [3] or the characterization of molecular chemical compositions [4,5]. Dynamic nuclear polarization (DNP), by which electron spin polarization is transferred to nuclear spins, is one of the promising methods to reach such a large enhancement of the signal.

Over the past decades, one of the outstanding challenges is the hyperpolarization of molecules in a solution [6–13]. In typical solutions, resonance-based polarization mechanisms commonly used in solid-state systems [14,15] are not effective due to the averaging of the electron-nuclear anisotropic interaction of the molecules by their rapid motion. Thus, cross-relaxation mechanisms such as the Overhauser effect [7,12,13] are typically applied to realize the polarization of fluids under ambient conditions. So far, the largest hyperpolarization is achieved for fast diffusing small molecules and is severely limited by the low thermal electron polarization in moderate magnetic fields. For example, for 2,2,6,6-tetramethyl-1-piperidine-1-oxyl (TEMPO), trityl, or biradical systems, the electron spin polarization amounts to only 0.08% for a magnetic field of $B = 0.36$ T [8,9]. In this Rapid Communication, we demonstrate that the use of optically hyperpolarized electron spins offers an exciting possibility for overcoming the limitation on the degree and rate of electron polarization. Specifically, nitrogen-vacancy (NV) centers in nanodiamonds (NDs) are excellent candidates for optically pumped hyperpolarization agents. The unique optical properties of the negatively charged nitrogen-vacancy center in nanodiamonds allow for over 90% electron spin polarization to be achieved in less than a microsecond by optical pumping [16] while exhibiting a relaxation time in the millisecond range even at room temperature [17]. Methods for the creation of high polarization in ^{13}C nuclear spins inside of bulk diamond have already been developed theoretically and demonstrated experimentally [18–24].

However, for NV centers the interaction correlation time τ_c [25] with nuclear spins in the surrounding molecules is atypically large, as τ_c scales with the square of the minimum distance with the nuclear spins, which is very large (a few nanometers) for NV centers in NDs. Thus, NV centers typically cannot be used with standard Overhauser cross-relaxation protocols. Here, we present a theoretical framework for polarizing molecules for systems with a large correlation time. Specifically, we apply resonance-based schemes, such as the solid effect, where under continuous microwave (MW) radiation the electron spin is driven to approach resonance with the nuclear spin of choice. Importantly, we will proceed to demonstrate that this scheme remains robust even in the presence of molecular motion and, unlike solid-state polarization methods, is tolerant to a relative large detuning from the resonance frequency.

We then consider a specific setup that realizes this protocol, where the NDs are immobilized in a hydrogel inside a flow channel, increasing τ_c, as well as limiting the nuclear spin relaxation due to electron spins to the polarization region. Detailed numerical simulations show that a very high nuclear spin polarization is achieved for volumes that are detectable in current NMR scanners.

Spin polarization via resonance-inclined transfer (SPRINT). We consider the polarization transfer induced by magnetic dipole-dipole coupling between an electron spin and all the surrounding solvent spins. Suppose, as shown

*qiong.chen@uni-ulm.de

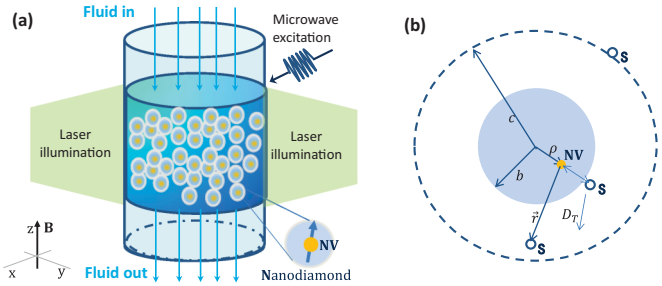

FIG. 1. (a) Schematic setup for polarization of nuclear spin in solution via NV centers in nanodiamonds. Fluid enters a channel containing a hydrogel cell with immobilized nanodiamonds for continuous DNP polarization. Optical polarization of the NV electron spins and microwave irradiation facilitates the polarization transfer to nuclear spins in the surrounding molecules. A permanent magnetic field B is applied along the z axis, which defines the coordinate system. (b) Illustration of the model parameters.

in Fig. 1(b), that the electron spin is located in the center of a ND, and we denote the distance of closest approach of the electron and nuclear spins by b. Denoting the molecular diffusion coefficient in solution with D_T, the interaction between the electron and solvent spins evolves in time with a characteristic correlation time $\tau_c = b^2/D_T$. c and ρ in Fig. 1(b) are related to an absorbing boundary and off-center effect, respectively, which are negligible in our case [see the Supplemental Material (SM) [26]].

In resonance-based DNP schemes, continuous MW radiation is applied to the electron spin [14,15], thus creating an "effective frequency" of the electron spin ω_E in the rotating frame. When the energy difference $\omega_0 = \omega_E - \omega_S$ between the effective frequency and the Larmor frequency ω_S of a specific nuclear spin species vanishes, a Hartmann-Hahn (H-H) resonance is achieved [27] and energy-conserving flip-flop transitions can occur between the electron and nuclear spins. Energy nonconserving flip-flip transitions are suppressed due to a large energy mismatch compared with the effective coupling between the electron and nuclear spin ($\omega_2 = \omega_E + \omega_S \gg g$). This difference between the flip-flop and flip-flip transitions leads to a net polarization transfer from electron spins to nuclear spins [26,28].

In the liquid phase, due to fast molecular diffusion, we can calculate perturbatively the transition probabilities W_i ($i = 0,2$) of the flip-flop transition rate $W_0 = \alpha_0 J(\omega_0)$ and flip-flip transition rate $W_2 = \alpha_0 J(\omega_2)$, in which the spectral density function is given by [26,29,30]

$$J(\omega) = \Gamma \,\mathrm{Re}\left[\frac{1+\frac{\sqrt{i\xi}}{4}}{1+\sqrt{i\xi}+\frac{4\left(\sqrt{i\xi}\right)^2}{9}+\frac{\left(\sqrt{i\xi}\right)^3}{9}}\right], \qquad (1)$$

where $\xi = \omega\tau_c$. α_0 is a constant involving the nuclear properties of the interacting system. Γ is the coefficient determined by system parameters, such as the minimum distance between the electron and solvent spins, the dipole-dipole coupling strength and translational diffusion coefficient, etc. (see the SM [26] for details). In simple solvents of low viscosity, such as protons in free water molecules, $D_T = D_w = 2 \times 10^{-9}$ m^2/s [31], and for a minimal distance of the electron and solvent spins of $b = 0.5$ nm, we find $\tau_c = b^2/D_T \sim 0.1$ ns. Then $\xi \ll 1$ is always satisfied for weak and moderate magnetic fields (i.e., $B < 1$ T), resulting in $\omega_S = (2\pi)16$ MHz for $B = 0.36$ T [see the blue dashed line in Fig. 2(a)]. Applying a MW driving fulfilling $\omega_E = \omega_S$ will lead to no appreciable difference between flip-flip and flip-flop effects, as $J(\omega_2) \cong J(\omega_0) \cong J(0)$ in general. This indifference of the transition rates to the energy mismatch is the main reason why resonance-based polarization schemes are not applicable to solutions with small τ_c. However, larger interaction correlation times achieved by increasing the distance $b = 5$ nm and decreasing the diffusion coefficient to induce $\tau_c = 100$ ns, as shown in the purple dotted line in Fig. 2(a), demonstrate a clear incline of net polarization towards a resonance condition. Using the same parameters discussed above, we now obtain $J(\omega_0) = J(0) \sim 1$ and $J(\omega_2) \sim 0$. Therefore, it is possible to achieve a polarization transfer in a solution with large τ_c by matching a H-H resonant condition. It is interesting to note that the relationship between our scheme and standard Overhauser cross polarization is similar to the sideband resolved regime and the Doppler (unresolved) regime in the laser cooling of cold trapped ions (see SM [26]). This results in a more efficient polarization transfer, which enables DNP via more distant electron spins, and with a weaker dipolar coupling to the nuclear spins.

The steady-state populations in the different nuclear spin states and the resulting polarization can then be determined from a detailed balance analysis. We find (here we ignore the relaxation times; see the SM [26] for a more detailed treatment)

$$P_s = -\frac{J(\omega_0) - J(\omega_2)}{J(\omega_0) + C_0 J(\omega_S) + J(\omega_2)}, \qquad (2)$$

in which $C_0 = 2\cot\varphi$ with $\cot\varphi = \epsilon/\Omega$ depending on the Rabi frequency of the MW radiation Ω and detuning of the MW field from the electron energy scale ϵ. Here, we assume that the electron spin is continuously pumped into a polarized state. Figure 2(b) shows the dependence of the achieved steady-state polarization on the detuning from the resonance condition and correlation time. As we are using the solid effect, we tune the MW field to achieve a resonant interaction as $\omega_S = \sqrt{\epsilon^2 + \Omega^2} = \omega_E = (2\pi)16$ MHz (see the SM [26]), where we have chosen $\epsilon = \Omega = (2\pi)8\sqrt{2}$ MHz. As shown in Fig. 2(a), for a large correlation time satisfying $\tau_c > 10$ ns, different rates between the flip-flop and flip-flip transitions induce a high steady-state polarization, quite similar to solid-state mechanisms. However, contrary to the solid-state phase, we can see that high steady-state polarization is achieved for a wide range of detuning from the resonance, as shown in Fig. 2(b). For example, for $\tau_c = 100$ ns, we observe a high steady-state polarization for a detuning as large as $\Delta' \sim (2\pi)10$ MHz. This is a unique characteristic of our theory in the liquid phase and different from the solid phase in which polarization transfer only occurs when the detuning is comparable to or smaller than the effective collective flip-flop coupling between the electron spin and nuclear spins [18,24]. Thus, this polarization by cross relaxation requires an inclination towards resonance, but the resonance condition does not have to be matched exactly.

Optical SPRINT with nanodiamonds. To model the dynamics of nuclear spin polarization transfer from NV centers in

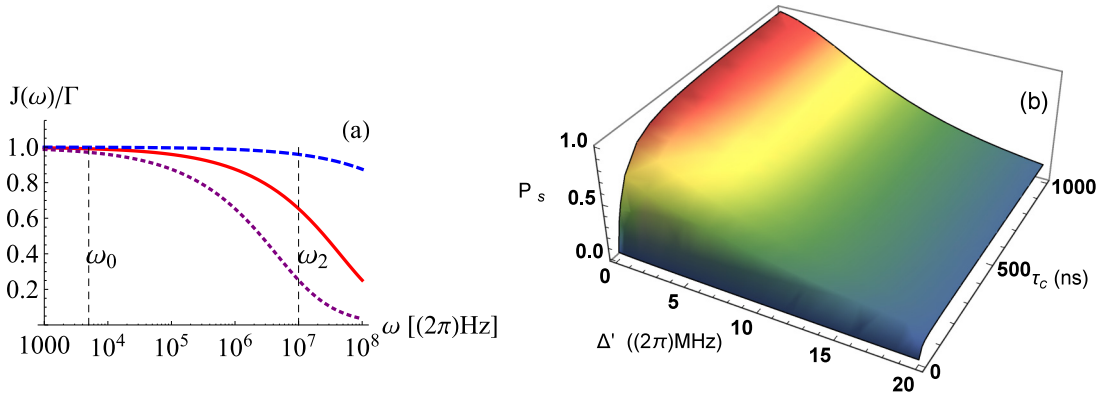

FIG. 2. (a) Spectra density function $J(\omega)/\Gamma$ as a function of frequency ω and interaction correlation time τ_c. The blue dashed, red solid, and purple dotted lines correspond to $\tau_c = 0.1$, 10, and 100 ns, respectively. (b) The steady-state polarization of the nuclear spins. $\omega_S = (2\pi)16$ MHz, $\epsilon_0 = \Omega = (2\pi)8\sqrt{2}$ MHz, and $\Delta' = \epsilon(\theta) - \epsilon_0$ is the detuning from the resonance point.

nanodiamonds to the protons in water, we consider a setup of Fig. 1(a). The solvent spins of the target molecules are pumped through a flow cell containing a hyperpolarization region in which nanodiamonds are immobilized in a hydrogel layer (see Fig. 1), causing a dipolar magnetic interaction between the NV spins and their surrounding solvent spins with a characteristic correlation time τ_c. Here, the electron spins of the NV centers will be strongly polarized by optical pumping, and the hydrogel provides a method for increasing the correlation time by reducing the diffusion rate of water molecules by a factor of 10^2–10^3 via controlling the mesh sizes and types of hydrogels [25].

A dc magnetic field $B \cong 0.36$ T whose direction defines the z axis of the laboratory frame is applied to the system. We assume $\gamma_e B \gg D$, where D is its zero-field splitting. As discussed in Ref. [18], in this regime the quantization axis of all NV centers is along $\vec{B}$, and the orientation of the symmetry axis of the NV center relative to $\vec{B}$ is uniformly distributed over the unit sphere. Here, θ denotes the angle between the NV center symmetry axis and the magnetic field axis. The random orientations of the NV centers cause two difficulties for the polarization transfer from the NV spin to the nuclear spins. First, a high optical polarization of the NV center spins is only achieved for the NV orientation near $\theta = 0^\circ$ and $\theta = 90^\circ$ by using 532 nm green laser illumination and, second, there is a variation of the energy splitting with θ (see SM [26]).

The rate of the polarization transfer is given by $W = W_0 - W_2 = \alpha_0(J(\omega_0) - J(\omega_2))$ [26]. Assuming the magnetic field is given by $B = 0.36$ T, $\omega_S = (2\pi)16$ MHz, for utilizing the effect of resonance in the current setup, we tune the MW frequency to achieve a resonant interaction for $\theta = 90^\circ$, and $\varepsilon_0 = \varepsilon(90^\circ) = \Omega = (2\pi)8\sqrt{2}$ MHz for matching a H-H resonance. Due to the strong dependence of the energy splitting between the spin levels on θ, for each NV spin with a specific $\epsilon(\theta)$, there is a detuning from resonance which leads to Δ' in Fig. 2(b). Here, we focus on the near resonant case around $\theta = 90^\circ$ because the same detuning leads to more NV spins to be involved in the $\theta = 90^\circ$ case as compared to the $\theta = 0^\circ$ case [e.g., $\Delta' < (2\pi)10$ MHz involves 5% NV spins in NDs in the former as compared to just 0.1% NV spins for the latter [18]]. We estimate the efficiency of our scheme by calculating the average polarization rate of the solvent spins $\overline{W}_{\text{eff}} = S^{-1}\int_S W P_C \cos\varphi dS$, with $P_C \cos\varphi$ the initial polarization of the corresponding NV spin according to the solid effect polarization mechanism [15] and S the solid angle covered.

For continuous optical pumping and $\theta = 90^\circ$ such that $P_C \simeq 0.5^2 = 0.25$ (corresponding to about 80% optical initialization), the dependence of the average polarization rate of the solvent spins for NDs of 5 nm radius on the ratio of the decreased translational diffusion k is shown in Fig. 3(a). Slow translational diffusion of the solvent molecules affects the polarization transfer in two competing ways: (i) increasing the correlation time to enhance the polarization transfer and (ii) decreasing the number of involved NV spins contributing to the polarization transfer (as slower diffusion leads to smaller accessible detuning from resonance for our scheme). Figure 3(a) predicts that the former will dominate (as expected, since the first effect is linear and the second sublinear). Thus, a fast polarization transfer can be achieved via a decrease of the

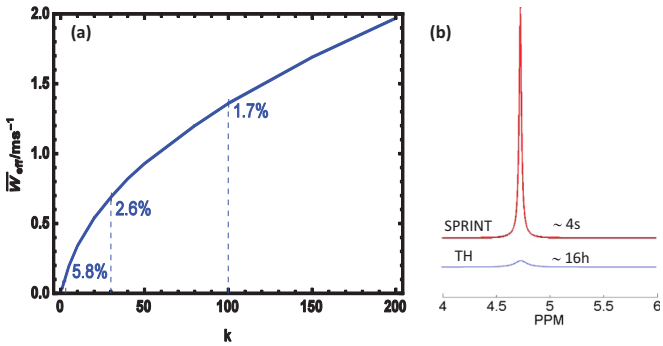

FIG. 3. (a) The averaged polarization rate of the solvent spins $\overline{W}_{\text{eff}}$. A $b = 5$ nm ND radius was assumed. $k = D_w/D_T$, with $D_w = 2 \times 10^{-9}$ m^2/s the diffusion coefficient in free water at room temperature, and D_T is the decreased translational diffusion coefficient. The percent of involved NV spins accounting for 90% of the polarization transfer is given for three different points. (b) The predicted water proton NMR spectrum by using the SPRINT technique (red) for a single shot NMR acquisition compared with 16 h accumulation of thermal polarization (blue) for $B = 0.36$ T.

diffusion rate. For example, when the size of the nanodiamond is $b = 5$ nm, $\overline{W}_{\text{eff}} \approx 0.04\ \text{ms}^{-1}$ for $k = 1$ and $\overline{W}_{\text{eff}} \approx 1.4\ \text{ms}^{-1}$ for $k = 100$.

The proposed setup is feasible with current experimental technology. Over the past decade, several experiments have realized polarization of flowing solvents by immobilized electron spins such as TEMPO and radicals in hydrogel layers [8,9,11] for $B \simeq 0.35$ T. Furthermore, it has been demonstrated that one can use functional groups on the diamond surface to replace these radicals with nanodiamonds in the hydrogel [32,33]. The nanodiamonds are immobilized in the hydrogel and it is not necessary to consider rotational diffusion. While the implementations employing either radicals or nanodiamonds are similar in spirit, it is crucial that the transparency of the hydrogel allows for the optical polarization of nanodiamonds, which has the potential to lead to a 300-fold increase of the achievable nuclear polarization over the implementations using radicals.

To estimate the total polarization of the solvent spins, we use an approximate formula for the steady-state bulk nuclear spin polarization of the solvent neglecting polarization diffusion, $P_{\text{lim}} \approx \frac{N_e}{N_p}\overline{W}_{\text{eff}}T_p$. Here, $\frac{N_e}{N_p}$ is the ratio of the number of the NV spins to proton spins in the polarization region (see SM), and T_p is the smaller of either the time the solvent is in contact with the hydrogel matrix or the solvent relaxation time. Suppose the flow channel is composed of a tube of a diameter of 0.3 mm, the size of the hydrogel layer is 10 mm, and the resulting volume is filled with NDs of 10 nm diameter such that they account for 12% of the total volume. Assuming, furthermore, that $k = 100$, we choose the flow rate of $v = 10^{-2}$ m/s (this flow rate is achieved with commercial pumps, where larger flow rates have been achieved in similar systems [11,34], and negligibly affects the molecular dynamics within τ_c) such that $T_p \sim T_1 \sim 1$ s. Given the density of protons in free water $66.6\ \text{nm}^{-3}$, we obtain $N_e/N_p \sim 4 \times 10^{-6}$, $\overline{W}_{\text{eff}} \approx 1.4\ \text{ms}^{-1}$, $T_p \approx 1$ s to arrive at a polarization of $P_{\text{lim}} \approx 0.6\%$ for the solution. This polarization, achieved in 1 s for a volume of 1 μl, is roughly 4700 times the thermal polarization and would already suffice for detection in a commercial NMR scanner [35]. This enhancement is illustrated in Fig. 3(b), where a simulated water proton NMR spectrum is compared for a single shot readout with DNP, and 16 h of thermal accumulation [37].

In the following, we briefly discuss various requirements and possible limitations in our setup. Optimal NV spin optical polarization in our setup requires around 10 μs mean repolarization time of the NVs in the 0.8 mm^3 volume. Fortunately, due to the small ND radius, Mie scattering does not limit the optical penetration depth in the 7 mm^3 volume for the ND concentration in the proposed setup (see SM). However, due to the efficient optical absorption by the NV centers which is partially converted to phonons, we expect heating of around 2 W for the 1 s a molecule spends in the polarization region for the chosen velocity. This heating power can be easily removed using active cooling. Even cooling only being performed from outside the sample tube (e.g., by fluid or gas cooling) will result in a maximal temperature difference of 25 °C [26] inside the sample, sufficiently low for experimental realization. Far from optical saturation, both the maximally achievable polarization and the heating depend linearly on $\frac{P_{\text{laser}}}{v}$, with P_{laser} denoting the incoming laser power. Thus, an increase in the maximal polarization would require a more efficient cooling scheme. A stringent limitation on the channel diameter is due to microwave absorption in water, which leads to a maximal capillary inner diameter of 1 mm [6], with no adverse effects for a diameter of 0.3 mm. Another important factor for the polarization transfer is the relaxation time T_1 of the protons in the hydrogel layer: As discussed in Ref. [25], this would depend on the material and mesh size in the gel, but can be assumed to be 0.3–2 s. As stated before, for optimal polarization and throughput, the flow speed should be chosen such that $T_p \sim T_1$. Molecules with a longer relaxation time could therefore achieve a higher maximal polarization in the same setup. As the polarization decays quickly back to thermal equilibrium, it is important to increase the flow speed outside the polarization zone, to reduce the time between polarization and detection. This can be achieved by, e.g., narrowing the channel diameter, intersecting with a fast-flowing channel, or by a mechanical shuttle.

We would like to stress that a wide variety of molecules can be polarized with the same methodology and setup, including ones with different nuclear spins (e.g., ^{13}C pyruvic acid for biomedical imaging) or of a larger size (e.g., biomacromolecules). More importantly, SPRINT can potentially be effective for nonoptical DNP systems, not involving nanodiamonds, for example, for DNP in high magnetic fields and/or with biomacromolecules (e.g., proteins). In these systems, if the interaction correlation time between the polarizing electron (e.g., in a radical) and the molecule can be increased, it would be relatively straightforward to apply our scheme. We anticipate that, with minor modifications, resonance-inclined transfer could be applied in combination with other solid-phase schemes, such as the cross effect.

Conclusion. We developed SPRINT, a resonance-inclined mechanism for the polarization of nuclear spins for large interaction correlation times in a solution. Importantly, this is a complementary method to the Overhauser effect, which is most efficient in the extreme narrowing regime. Due to molecular motion, our scheme is tolerant to a relatively large deviation from the resonant frequency. Furthermore, we propose a polarization setup using NV centers in nanodiamonds held in a hydrogel inside a flow cell which combines the advantages of this scheme with optical electron polarization. Under realistic experimental conditions, a polarization enhancement of 4700 times is observed. Our resonance-inclined scheme applies in a wide variety of DNP realizations, especially with biomacromolecules or large magnetic fields.

Acknowledgments. We thank Yuzhou Wu, Pelayo Fernandez Acebal, Oded Rosolio, Benedikt Tratzmiller, and Martin Bruderer for insightful discussions. This work was supported by an Alexander von Humboldt professorship, the ERC Synergy Grant BioQ, the ERC POC grant NDI, an IQST Ph.D. Fellowship, the EU projects SIQS, DIADEMS, and HYPERDIAMOND, as well as the DFG CRC TR 21 and Volkswagenstiftung.

Q.C. and I.S. contributed equally to this work.

[1] F. Bloch, W. W. Hansen, and M. Packard, Phys. Rev. **70**, 474 (1946).
[2] E. M. Purcell, H. C. Torrey, and R. V. Pound, Phys. Rev. **69**, 37 (1946).
[3] M. Law, S. Cha, E. A. Knopp, G. Johnson, J. Arnett, and A. W. Litt, Radiology **222**, 715 (2002).
[4] C. Luchinat and G. Parigi, Appl. Magn. Reson. **34**, 379 (2008).
[5] I. Bertini, Y. K. Gupta, C. Luchinat, G. Parigi, C. Schlörb, and H. Schwalbe, Angew. Chem. **117**, 2263 (2005).
[6] Y. E. Nesmelov, A. Gopinath, and D. D. Thomas, J. Magn. Reson. **167**, 138 (2004).
[7] A. Abragam, *The Principles of Nuclear Magnetism*, International Series of Monographs on Physics No. 32 (Oxford University Press, Oxford, UK, 1961).
[8] E. R. McCarney, B. D. Armstrong, M. D. Lingwood, and S. Han, Proc. Natl. Acad. Sci. USA **104**, 1754 (2007).
[9] E. R. McCarney and S. Han, J. Magn. Reson. **190**, 307 (2008).
[10] C.-G. Joo, K.-N. Hu, J. A. Bryant, and R. G. Griffin, J. Am. Chem. Soc. **128**, 9428 (2006).
[11] S. Ebert, A. Amar, C. Bauer, M. Kölzer, P. Blömler, H. W. Spiess, D. Hinderberger, and K. Münnemann, Appl. Magn. Reson. **43**, 195 (2012).
[12] W. Anderson and R. Freeman, J. Chem. Phys. **37**, 85 (1962).
[13] S. Gabl, O. Steinhauser, and H. Weingärtner, Angew. Chem. **125**, 9412 (2013).
[14] A. Abragam and M. Goldman, Rep. Prog. Phys. **41**, 395 (1978).
[15] W. T. Wenckebach, Appl. Magn. Reson. **34**, 227 (2008).
[16] N. B. Manson, J. P. Harrison, and M. J. Sellars, Phys. Rev. B **74**, 104303 (2006).
[17] F. Jelezko, T. Gaebel, I. Popa, M. Domhan, A. Gruber, and J. Wrachtrup, Phys. Rev. Lett. **93**, 130501 (2004).
[18] Q. Chen, I. Schwarz, F. Jelezko, A. Retzker, and M. B. Plenio, Phys. Rev. B **92**, 184420 (2015).
[19] J. M. Cai, F. Jelezko, M. B. Plenio, and A. Retzker, New J. Phys. **15**, 013020 (2013).
[20] J. P. King, K. Jeong, C. C. Vassiliou, C. S. Shin, R. H. Page, C. E. Avalos, Hai-Jing Wang, and A. Pines, Nat. Commun. **6**, 8965 (2015).
[21] G. A. Álvarez, C. O. Bretschneider, R. Fischer, P. London, H. Kanda, S. Onoda, J. Isoya, D. Gershoni, and L. Frydman, Nat. Commun. **6**, 8456 (2015).
[22] J. M. Cai, B. Naydenov, R. Pfeiffer, L. P. McGuinness, K. D. Jahnke, F. Jelezko, M. B. Plenio, and A. Retzker, New J. Phys. **14**, 113023 (2012).
[23] J. M. Cai, A. Retzker, F. Jelezko, and M. B. Plenio, Nat. Phys. **9**, 168 (2013).
[24] P. London, J. Scheuer, J. M. Cai, I. Schwarz, A. Retzker, M. B. Plenio, M. Katagiri, T. Teraji, S. Koizumi, J. Isoya, R. Fischer, L. P. McGuinness, B. Naydenov, and F. Jelezko, Phys. Rev. Lett. **111**, 067601 (2013).
[25] Y. E. Shapiro, Prog. Polym. Sci. **36**, 1184 (2011).
[26] See Supplemental Material at http://link.aps.org/supplemental/10.1103/PhysRevB.93.060408 for the detailed calculations.
[27] S. Hartmann and E. Hahn, Phys. Rev. **128**, 2042 (1962).
[28] I. Solomon, Phys. Rev. **99**, 559 (1955).
[29] L. P. Hwang and J. H. Freed, J. Chem. Phys. **63**, 4017 (1975).
[30] B. Halle, J. Chem. Phys. **119**, 12372 (2003).
[31] K. Krynicki, C. D. Green, and D. W. Sawyer, Faraday Discuss. Chem. Soc. **66**, 199 (1978).
[32] H. Huang, E. Pierstorff, E. Osawa, and D. Ho, Nano Lett. **7**, 3305 (2007).
[33] E. von Haartman, H. Jiang, A. A. Khomich, J. Zhang, S. A. Burikov, T. A. Dolenko, J. Ruokolainen, H. Gu, O. A. Shenderova, I. I. Vlasov, and J. M. Rosenholm, J. Mater. Chem. B **1**, 2358 (2013).
[34] The pressure difference required for sustaining this flow rate in the 1 mm^3 hydrogel layer is negligible, on the order of 1 Pa.
[35] It is interesting to note that a recently proposed setup for polarization of fluids in a microfluidic diamond channel achieves a similar degree of polarization, but due to the limitations on the microfluidic channel size in the proposed protocol, it requires over 1000 parallel channels for polarizing 1 μl of solvent within 1 s [36].
[36] D. Abrams, M. E. Trusheim, D. R. Englund, M. D. Shattuck, and C. A. Meriles, Nano Lett. **14**, 2471 (2014).
[37] A. M. Castillo, L. Patiny, and J. Wist, J. Magn. Reson. **209**, 123 (2011).